

## Supporting Information

# High surface area of carbonaceous Cr<sub>2</sub>GaC composite microspheres synthesized by sol-gel chemistry

*Jordan Sinclair<sup>1</sup>, Jan P. Siebert<sup>1</sup>, Matt Flores<sup>1</sup>, David Ciota<sup>1</sup>, Don-Kyun Seo<sup>1</sup>, \*Christina S. Birkel<sup>1,2</sup>*

<sup>1</sup>*School of Molecular Sciences, Arizona State University, Tempe AZ-85282, USA.*

<sup>2</sup>*Department of Chemistry and Biochemistry, Technische Universitaet Darmstadt, 64287 Darmstadt, Germany*

*Email: Christina.Birkel@asu.edu*

## Sol-Gel Synthesis of Cr<sub>2</sub>GaC-based Microspheres

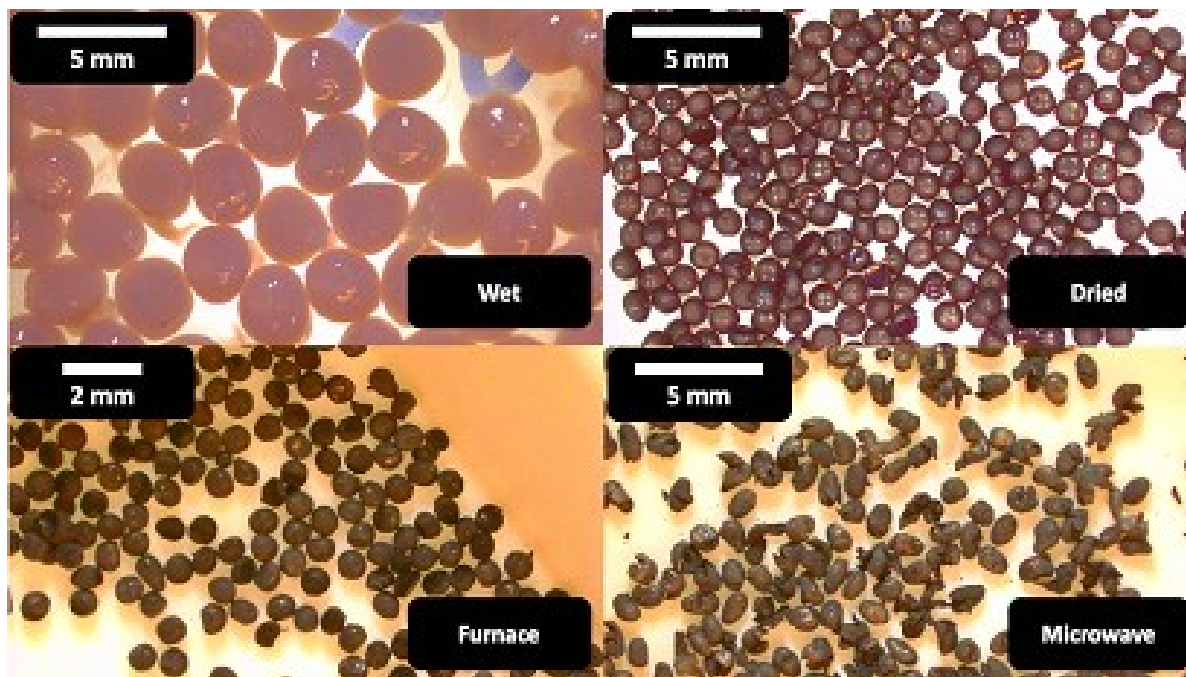


**Figure S1.** Images of the 17-gauge derived Cr<sub>2</sub>GaC Microspheres in four different states (wet, dried, furnace treated, and microwave treated)

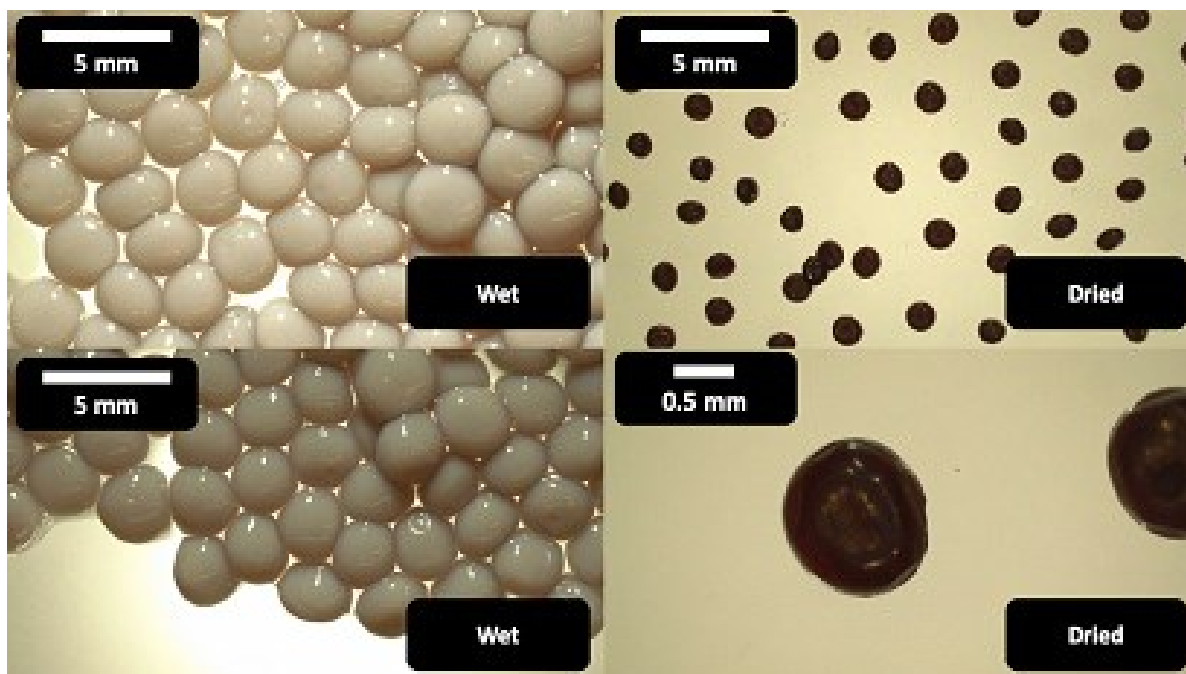


**Figure S2.** Images of the 18-gauge derived Cr<sub>2</sub>GaC Microspheres in two different states (wet, dried)

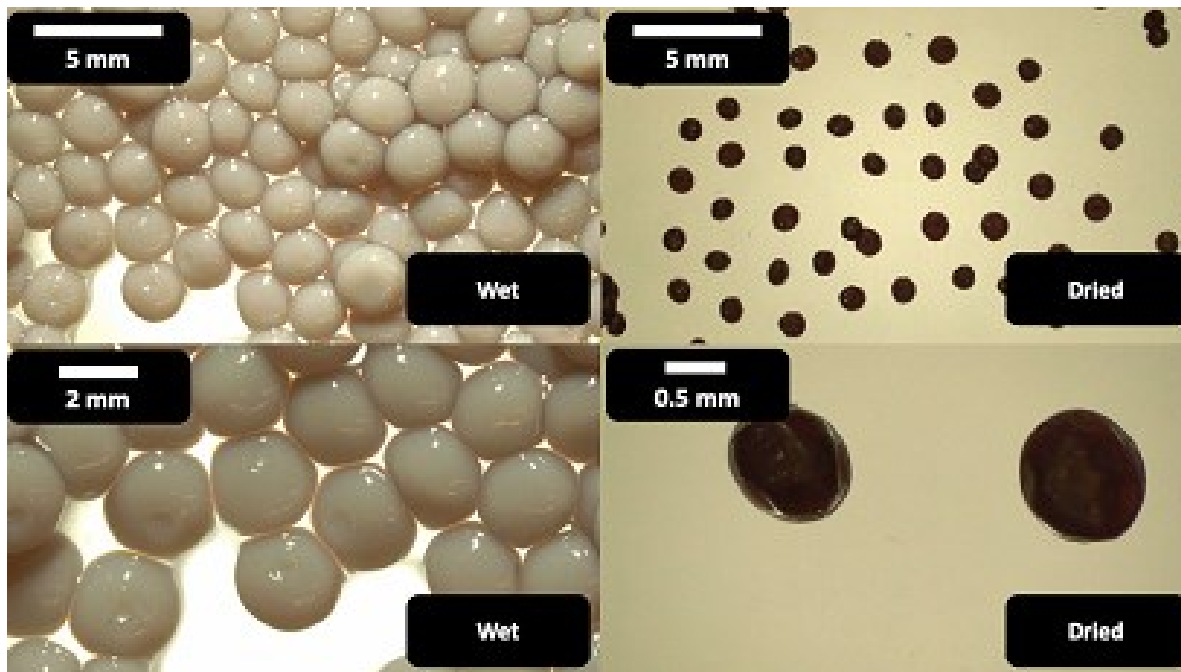


**Figure S3.** Images of the 20-gauge derived  $\text{Cr}_2\text{GaC}$  Microspheres in two different states (wet, dried)

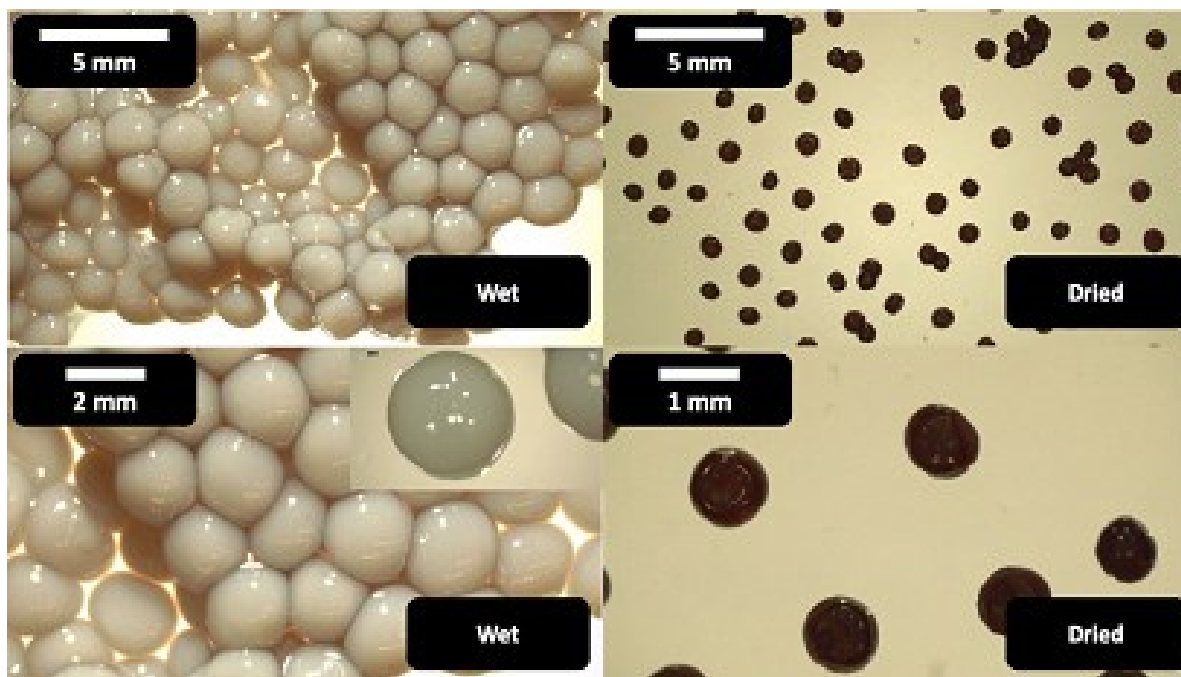


**Figure S4.** Images of the 23-gauge derived  $\text{Cr}_2\text{GaC}$  Microspheres in two different states (wet, dried)

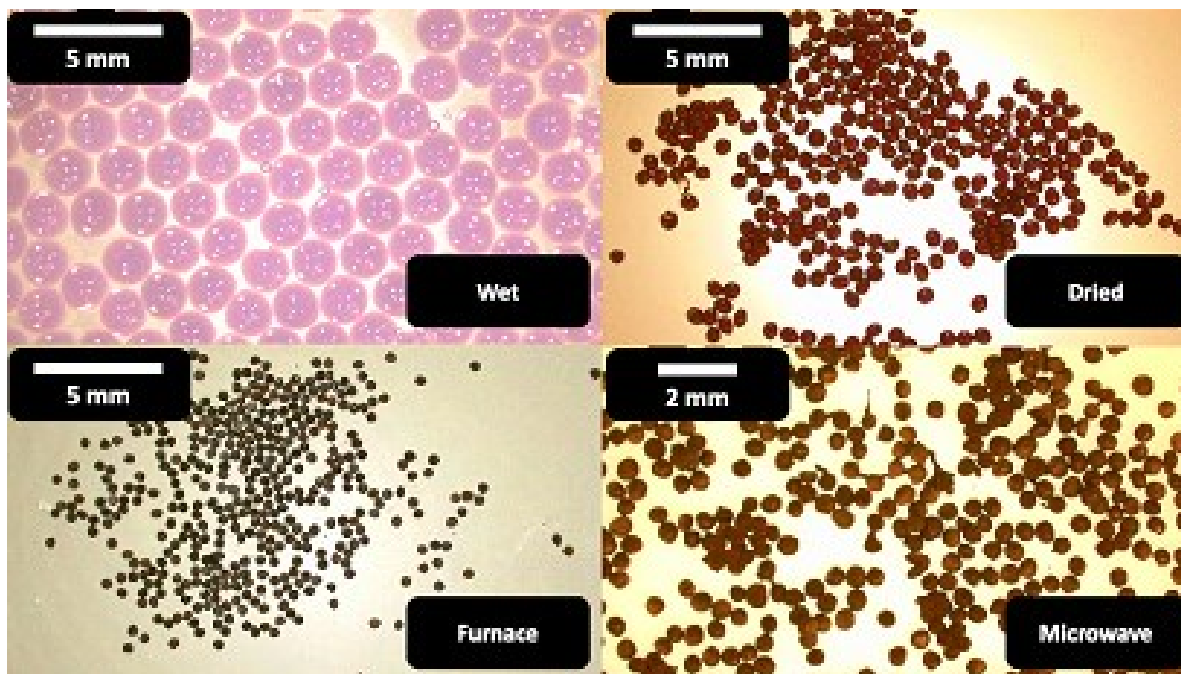


**Figure S5.** Images of the 26-gauge derived  $\text{Cr}_2\text{GaC}$  Microspheres in four different states (wet, dried, furnace treated, and microwave treated)

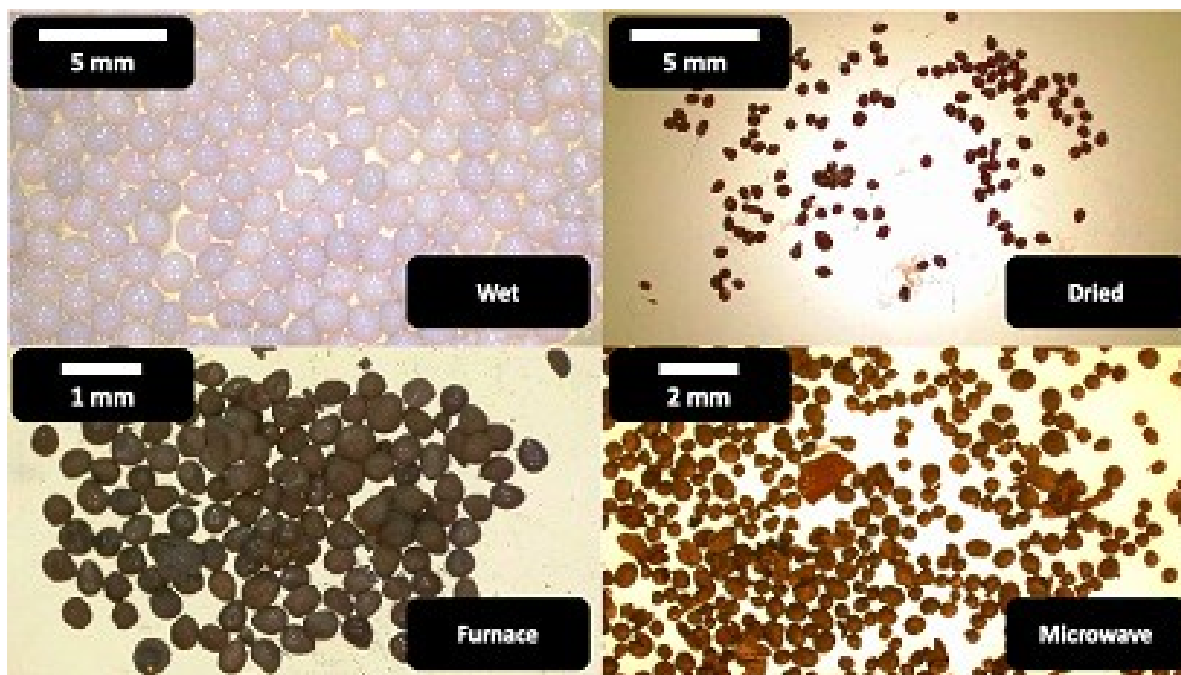


**Figure S6.** Images of the 30-gauge derived  $\text{Cr}_2\text{GaC}$  Microspheres in four different states (wet, dried, furnace treated, and microwave treated)

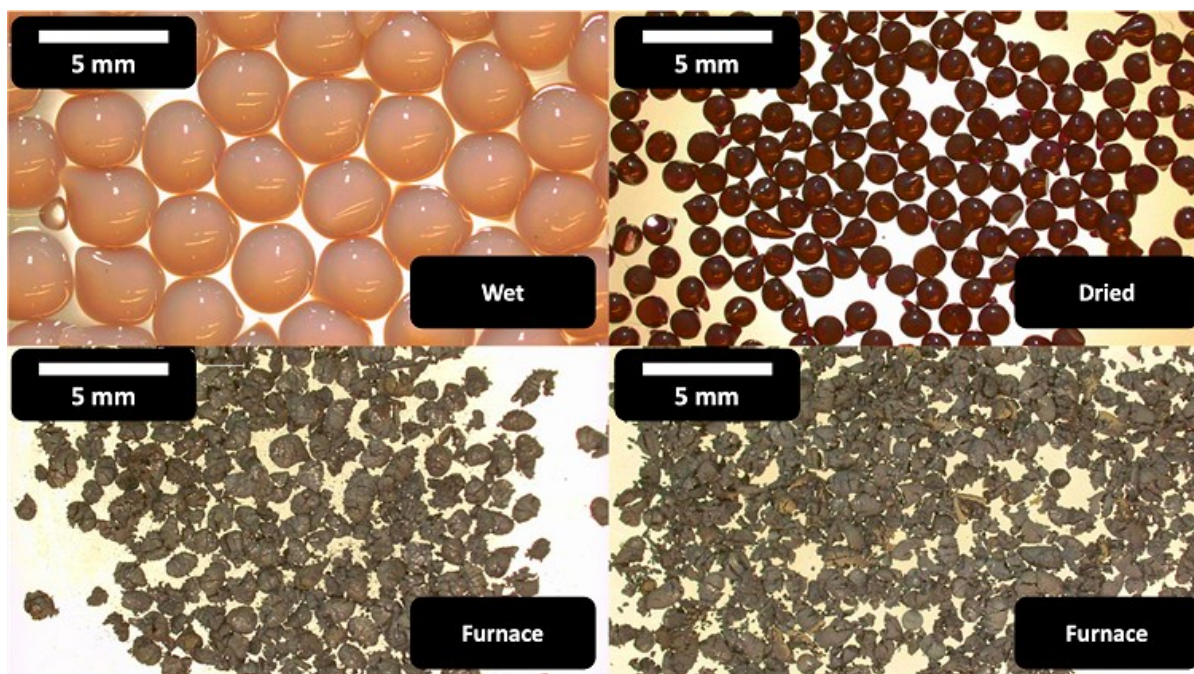


**Figure S7.** Images of the 14-gauge derived  $\text{Cr}_2\text{GaC}$  Microspheres in three different states (wet, dried, and furnace treated)

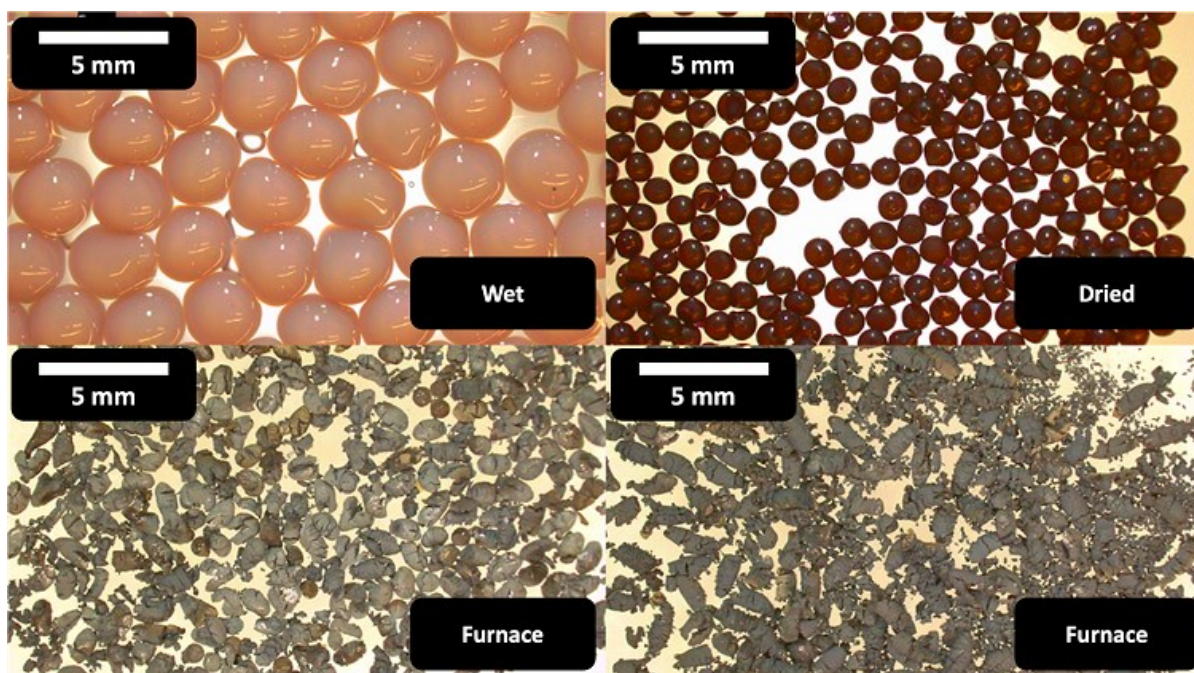


**Figure S8.** Images of the 16-gauge derived  $\text{Cr}_2\text{GaC}$  Microspheres in three different states (wet, dried, and furnace treated)

Performing the  $\text{Cr}_2\text{GaC}$  microsphere synthesis there is a clear threshold where the spheres lose the ability to retain their spherical nature. The 14- and 16-gauge sizes (1.77 mm and 1.35 mm) experience a large degree of tailing when adding spheres of this size to the dilute  $\text{NH}_4\text{OH}$ . This is shown clearly in Figure S7-S8 when observing the spheres in a dried state. Upon combustion of

the 14 and 16 gauge the spheres appear completely destroyed, Figure S7-S8, observing spheres in the furnace heated treated state. 17-gauge derived spheres are the cutoff for microsphere production as the size of the sphere is sufficient to avoid spherical collapse. This however, is not a majority of the spheres as cracks prevalent upon closer inspection in the furnace and microwave synthesis routes, Figure S1. 18-gauge microspheres exhibit no spherical collapse and showcase the ability to handle the outgassing of different species that result from sol-gel synthesis.

### BET Report, ILP Microwave, BJH Pore Diameter Analysis, and Mass Data

**Table 1. BET specific surface area and average pore size of all Cr<sub>2</sub>GaC microspheres obtained after microwave annealing with varying needle gauge sizes.**

Gauge Size (mm)	Bet Surface Area (m <sup>2</sup> /g)	T-Plot Micropore Area (m <sup>2</sup> /g)	T-Plot External Area (m <sup>2</sup> /g)	Micropore Volume (cm <sup>3</sup> /g)
1.4	467	286	181	0.132
1.27	465	245	219	0.112
0.91	462	266	196	0.122
0.64	429	248	181	0.114
0.46	447	222	226	0.101
0.31	445	241	204	0.110

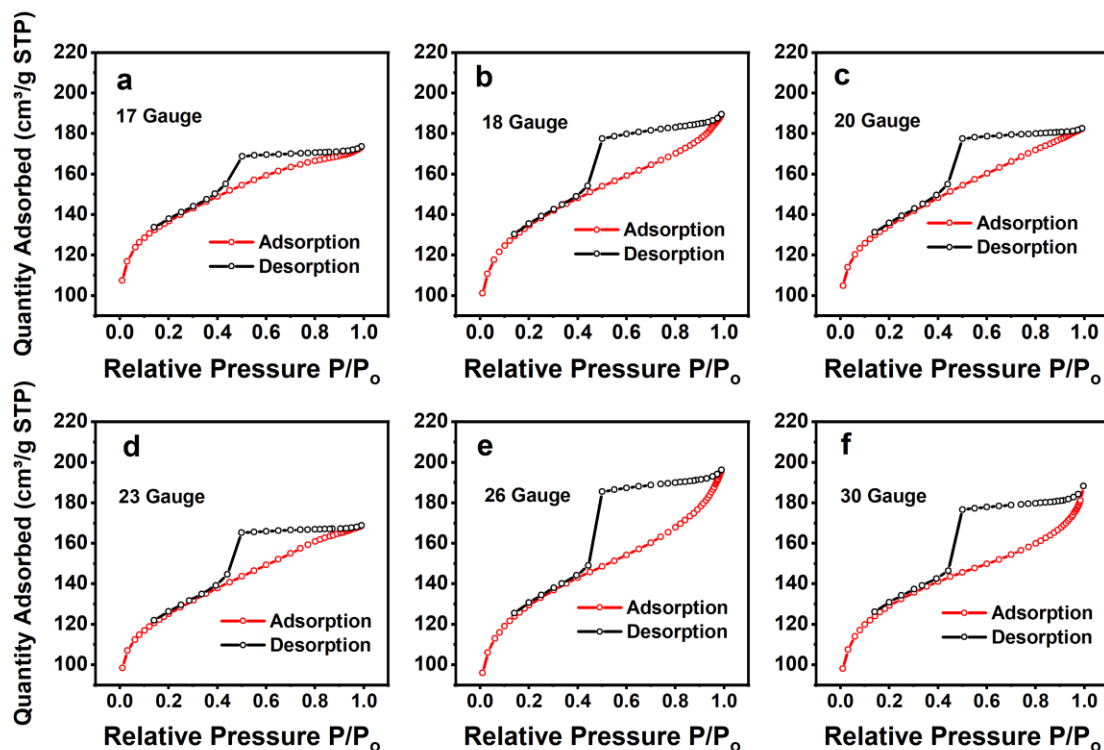


**Figure S9.** Isotherm Linear Plots of Cr<sub>2</sub>GaC microspheres obtained after microwave annealing using (a) 17-Gauge (b) 18-Gauge (c) 20-Gauge (d) 23-Gauge (e) 26-Gauge (f) 30-Gauge.

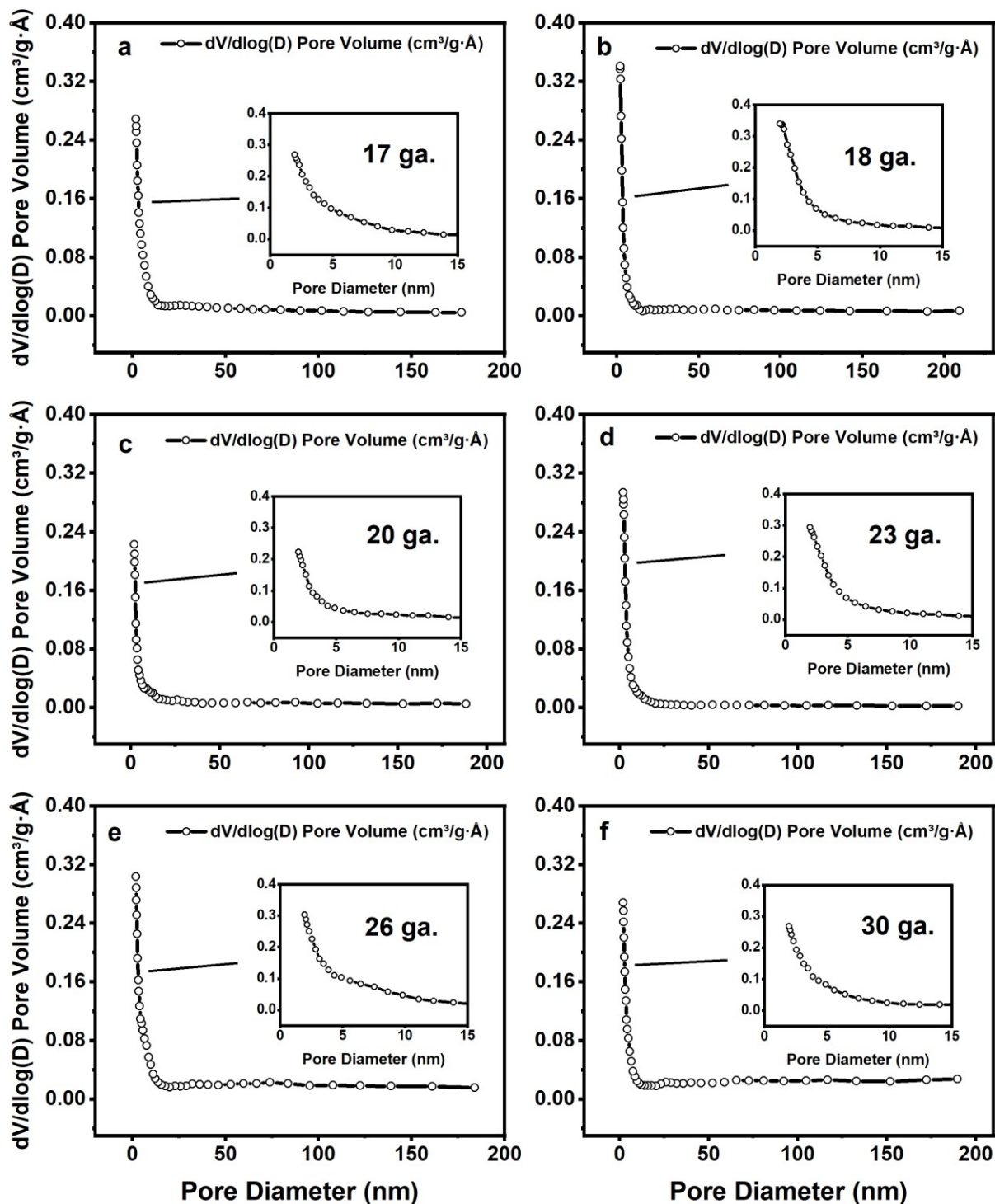


**Figure S10.** Adsorption Branch BJH Pore Analysis plots of furnace synthesized  $\text{Cr}_2\text{GaC}$  microsphere. All sizes range are (a) 17-gauge (b) 18-gauge (c) 20-gauge (d) 23-gauge (e) 26-gauge (f) 30-gauge (1.4-0.31 mm).

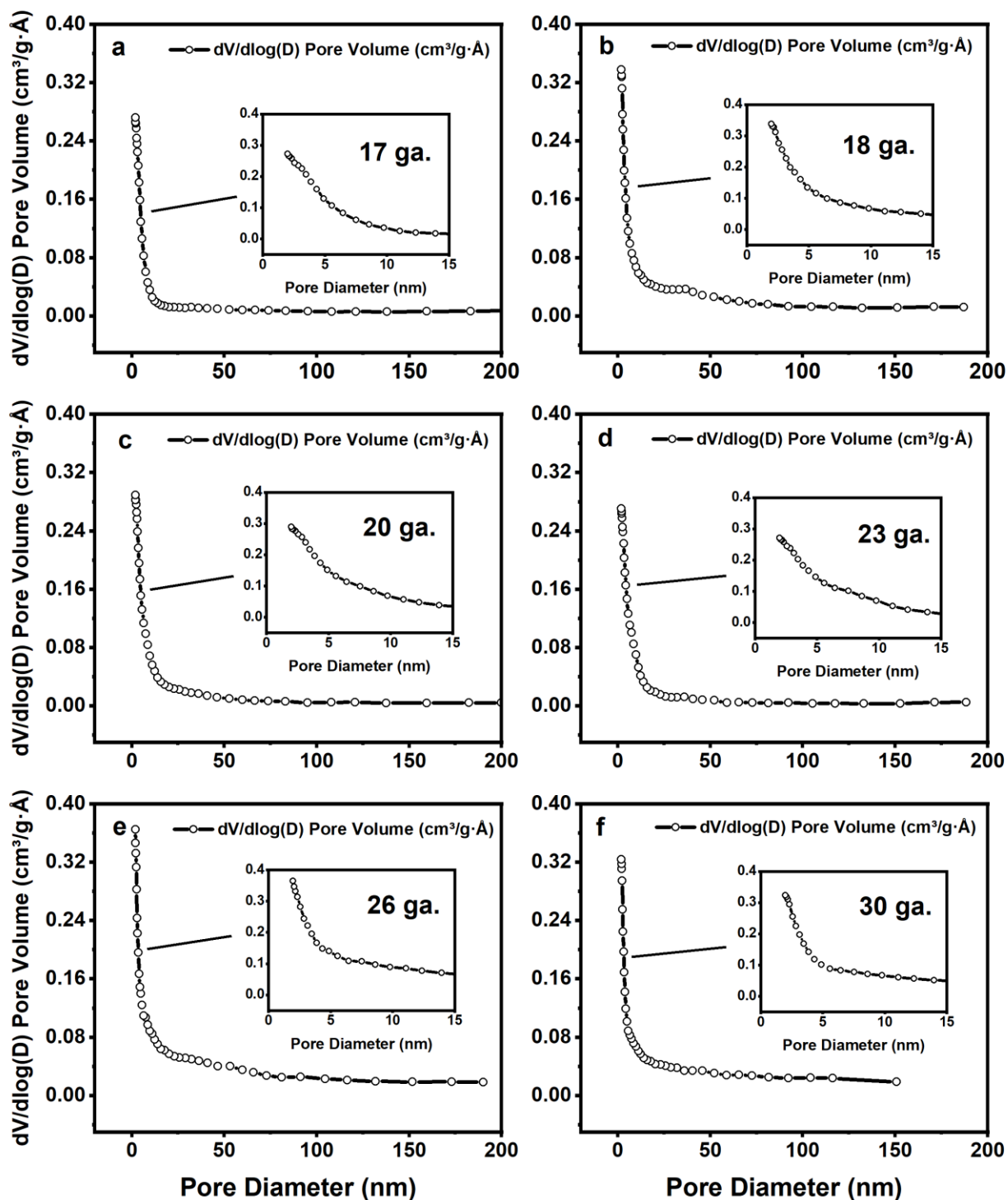


**Figure S11.** Adsorption Branch BJH Pore Analysis plots of microwave synthesized  $\text{Cr}_2\text{GaC}$  microsphere. All sizes range are (a) 17-gauge (b) 18-gauge (c) 20-gauge (d) 23-gauge (e) 26-gauge (f) 30-gauge (1.4-0.31 mm).)



## Furnace Synthesized Microsphere Rietveld Refinements

All Powder X-Ray Diffraction data was produced utilizing a Bruker D2 Phaser (2<sup>nd</sup> Generation), equipped with Cu K <sub>$\alpha$ 1,2</sub> radiation and a 1D SDD detector. To perform the Rietveld refinements with a very high-signal-to-noise ratio, 8 data sets from each sample was experimentally measured and then computationally combined. All refinements were performed in Topas<sup>1</sup>, all theoretical profiles and CIFs were obtained from ICSD<sup>2</sup> and Pearson Database<sup>3</sup>. Background and sample displacement factors were considered utilizing a 10<sup>th</sup> order polynomial initially and worked all the way up to a 15<sup>th</sup> order polynomial if plausible. The lattice parameters and scale were then refined taking advantage of a modified Thompson-Cox-Hastings pseudo-Voigt function (pv-TCHZ). Atom positionings, thermal displacement parameters (Beq), and occupancies were then refined. Values  $\geq 0$  for the Beq and  $\leq 1$  for the occupancies were accepted as reasonable for the Rietveld fit. Tables S2– S13 showcase the refinement parameters of the Cr<sub>2</sub>GaC microspheres. This includes both the furnace and microwaved synthesized variations. Figures S12-S13 display the fits, percentages of phases, R<sub>exp</sub>, and R<sub>wp</sub>. GOF values are also displayed in Tables S2-S13.

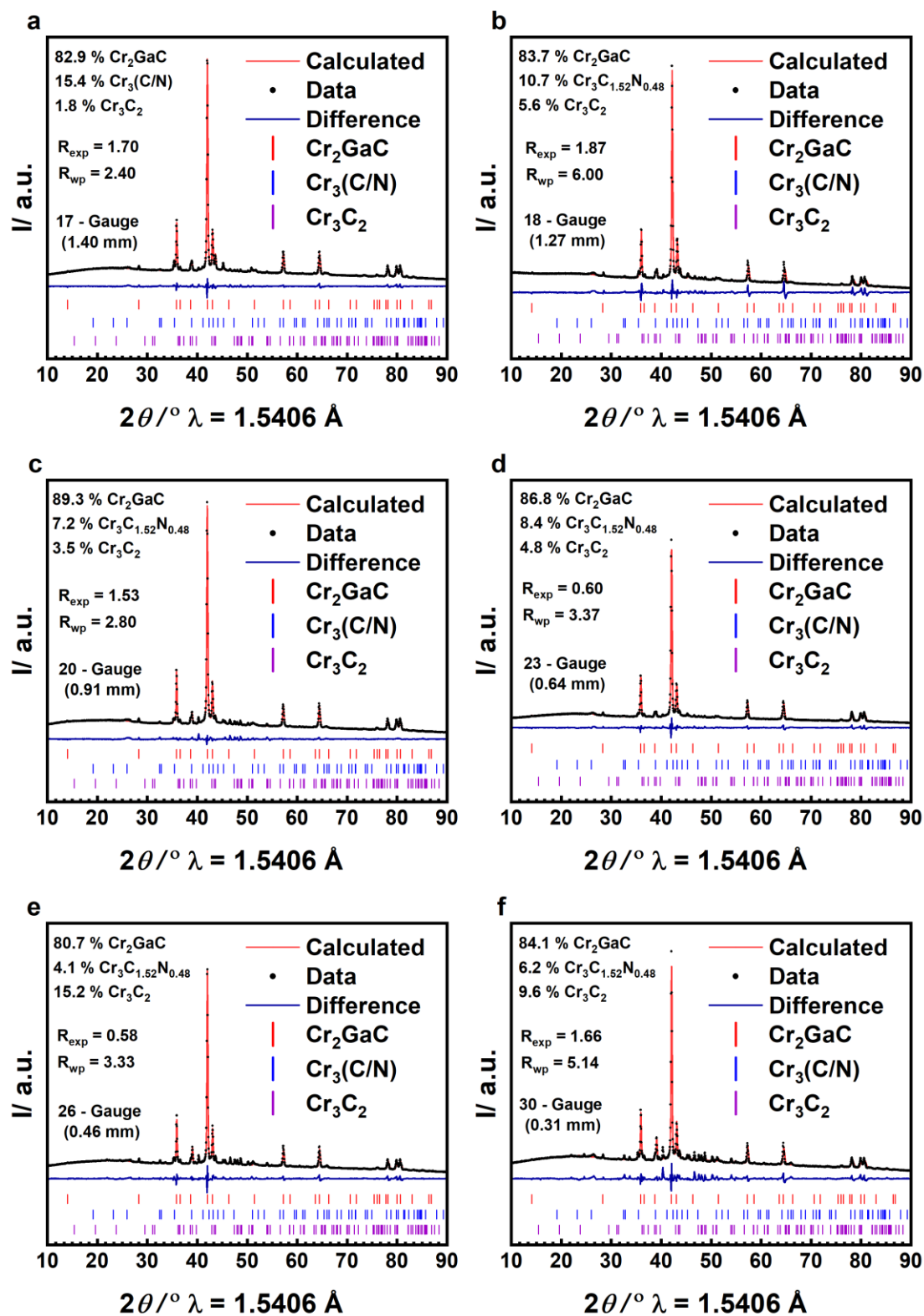


**Figure S12.** Rietveld Refinement Plots and percentages of all furnace Cr<sub>2</sub>GaC microspheres (a) 17-gauge (b) 18-gauge (c) 20-gauge (d) 23-gauge (e) 26-gauge (f) 30-gauge (1.4-0.31 mm).

**Table S2:** Rietveld refinement parameters of furnace-derived 17-gauge spheres

<b>Cr<sub>2</sub>GaC ( 82.9 (5) wt%)</b>	<b>x</b>	<b>y</b>	<b>z</b>	<b>Occupancy</b>	<b>Beq</b>
Cr1	0.3333	0.6667	0.8690	1.00	2.115
Ga1	0.3333	0.6667	0.7500	1.00	2.997
Cl	0.0000	0.0000	0.0000	1.00	1
a /Å				2.89005 (4)	
c /Å				12.6051 (3)	
a /Å				3.0770 <sup>3</sup>	
c /Å				10.9100 <sup>3</sup>	
R <sub>Bragg</sub>				0.705	
GOF				1.42	

**Table S3:** Rietveld refinement parameters of furnace-derived 18-gauge spheres

<b>Cr<sub>2</sub>GaC ( 83.7 (13) wt%)</b>	<b>x</b>	<b>y</b>	<b>z</b>	<b>Occupancy</b>	<b>Beq</b>
Cr1	0.3333	0.6667	0.8690	1.00	2.115
Ga1	0.3333	0.6667	0.7500	1.00	2.997
Cl	0.0000	0.0000	0.0000	1.00	1
a /Å				2.88059 (11)	
c /Å				12.5694 (9)	
a /Å				3.0770 <sup>3</sup>	
c /Å				10.9100 <sup>3</sup>	
R <sub>Bragg</sub>				2.177	
GOF				3.21	

**Table S4:** Rietveld refinement parameters of furnace-derived 20-gauge spheres

<b>Cr<sub>2</sub>GaC ( 89.3 (7) wt%)</b>	<b>x</b>	<b>y</b>	<b>z</b>	<b>Occupancy</b>	<b>Beq</b>
Cr1	0.3333	0.6667	0.8690	1.00	2.115
Ga1	0.3333	0.6667	0.7500	1.00	2.997
Cl	0.0000	0.0000	0.0000	1.00	1
a /Å				2.89128 (4)	
c /Å				12.6111 (3)	
a /Å				3.0770 <sup>3</sup>	
c /Å				10.9100 <sup>3</sup>	
R <sub>Bragg</sub>				0.833	
GOF				1.83	

**Table S5:** Rietveld refinement parameters of furnace-derived 23-gauge spheres

<b>Cr<sub>2</sub>GaC ( 86.8 (9) wt%)</b>	<b>x</b>	<b>y</b>	<b>z</b>	<b>Occupancy</b>	<b>Beq</b>
Cr1	0.3333	0.6667	0.8690 (3)	1.00	2.110 (13)
Ga1	0.3333	0.6667	0.7500	1.00	3.00 (17)
Cl	0.0000	0.0000	0.0000	1.00	1.0 (4)
a /Å				2.88917 (6)	

c /Å	12.5988 (4)
a /Å	3.0770 <sup>3</sup>
c /Å	10.9100 <sup>3</sup>
R <sub>Bragg</sub>	0.832
GOF	5.60

**Table S6:** Rietveld refinement parameters of furnace-derived 26-gauge spheres

<b>Cr<sub>2</sub>GaC ( 80.7 (9) wt%)</b>	<b>x</b>	<b>y</b>	<b>z</b>	<b>Occupancy</b>	<b>Beq</b>
Cr1	0.3333	0.6667	0.8690	1.00	2.115
Ga1	0.3333	0.6667	0.7500	1.00	2.997
C1	0.0000	0.0000	0.0000	1.00	1
a /Å				2.88975 (6)	
c /Å				12.5995 (5)	
a /Å				3.0770 <sup>3</sup>	
c /Å				10.9100 <sup>3</sup>	
R <sub>Bragg</sub>				0.764	
GOF				5.77	

**Table S7:** Rietveld refinement parameters of furnace-derived 30-gauge spheres

<b>Cr<sub>2</sub>GaC ( 84.1 (12) wt%)</b>	<b>x</b>	<b>y</b>	<b>z</b>	<b>Occupancy</b>	<b>Beq</b>
Cr1	0.3333	0.6667	0.8690	1.00	2.115
Ga1	0.3333	0.6667	0.7500	1.00	2.997
C1	0.0000	0.0000	0.0000	1.00	1
a /Å				2.88817 (10)	
c /Å				12.5948 (8)	
a /Å				3.0770 <sup>3</sup>	
c /Å				10.9100 <sup>3</sup>	
R <sub>Bragg</sub>				0.675	
GOF				3.10	

## Microwave Synthesized Microsphere Rietveld Refinements

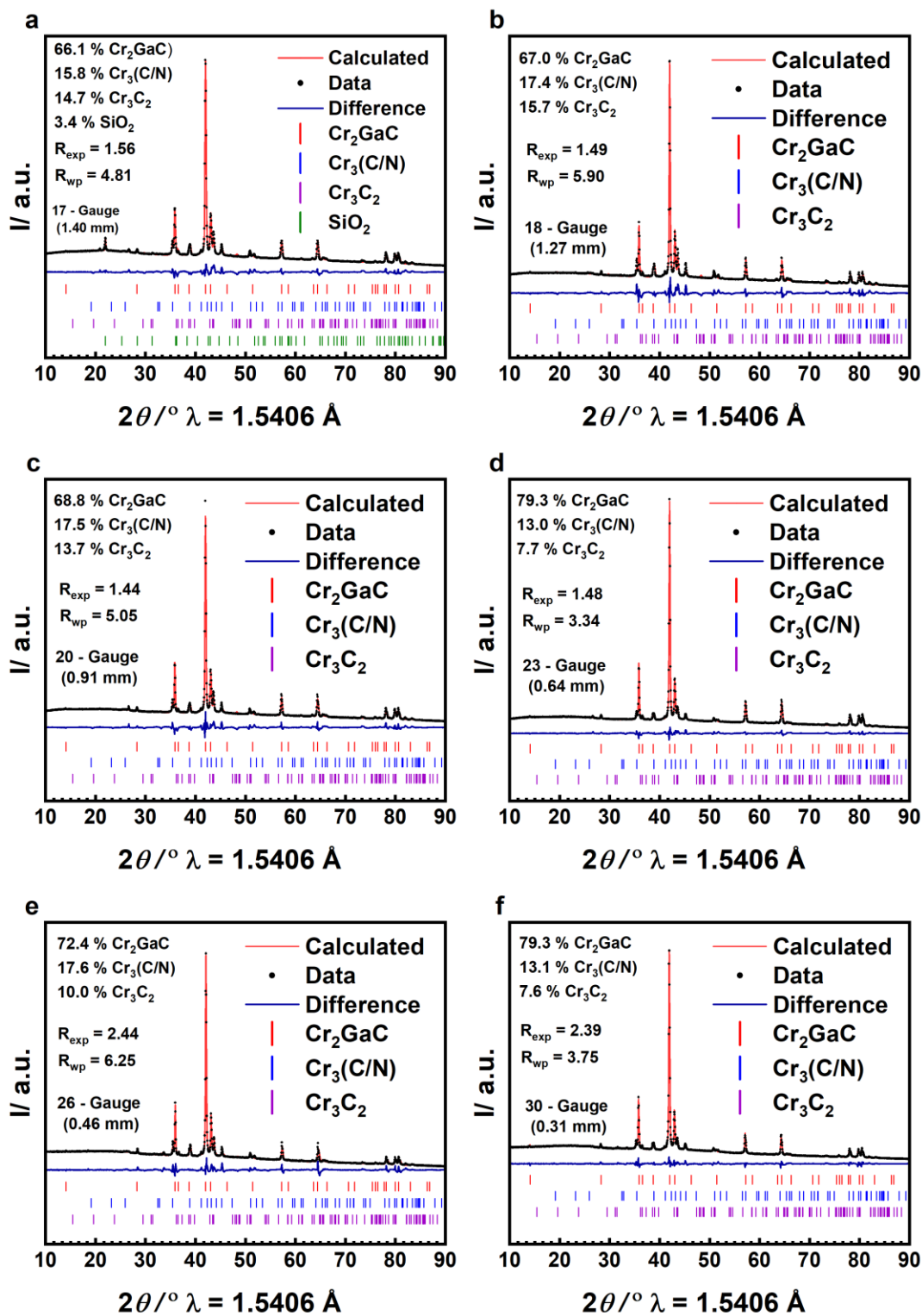


**Figure S13.** Rietveld Refinement Plots and percentages of all microwave Cr<sub>2</sub>GaC microspheres (a) 17-gauge (b) 18-gauge (c) 20-gauge (d) 23-gauge (e) 26-gauge (f) 30-gauge (1.4-0.31 mm).

**Table S8:** Rietveld refinement parameters of microwave-derived 17-gauge spheres

<b>Cr<sub>2</sub>GaC</b> (66.1 (11) wt%)	<b>x</b>	<b>y</b>	<b>z</b>	<b>Occupancy</b>	<b>Beq</b>
Cr1	0.3333	0.6667	0.8690	1.00	2.115
Ga1	0.3333	0.6667	0.7500	1.00	2.997
Cl	0.0000	0.0000	0.0000	1.00	1
a /Å				2.88956 (13)	
c /Å				12.5973 (9)	
a /Å				3.0770 <sup>3</sup>	
c /Å				10.9100 <sup>3</sup>	
R <sub>Bragg</sub>				1.857	
GOF				3.07	

**Table S9:** Rietveld refinement parameters of microwave-derived 18-gauge spheres

<b>Cr<sub>2</sub>GaC</b> ( 67.0 (14) wt%)	<b>x</b>	<b>y</b>	<b>z</b>	<b>Occupancy</b>	<b>Beq</b>
Cr1	0.3333	0.6667	0.8690	1.00	2.115
Ga1	0.3333	0.6667	0.7500	1.00	2.997
Cl	0.0000	0.0000	0.0000	1.00	1
a /Å				2.88924 (12)	
c /Å				12.5959 (8)	
a /Å				3.0770 <sup>3</sup>	
c /Å				10.9100 <sup>3</sup>	
R <sub>Bragg</sub>				2.396	
GOF				3.96	

**Table S10:** Rietveld refinement parameters of microwave-derived 20-gauge spheres

<b>Cr<sub>2</sub>GaC</b> ( 68.8 (12) wt%)	<b>x</b>	<b>y</b>	<b>z</b>	<b>Occupancy</b>	<b>Beq</b>
Cr1	0.3333	0.6667	0.8690	1.00	2.115
Ga1	0.3333	0.6667	0.7500	1.00	2.997
Cl	0.0000	0.0000	0.0000	1.00	1
a /Å				2.89030 (9)	
c /Å				12.6013 (7)	
a /Å				3.0770 <sup>3</sup>	
c /Å				10.9100 <sup>3</sup>	
R <sub>Bragg</sub>				2.088	
GOF				3.50	

**Table S11:** Rietveld refinement parameters of microwave-derived 23-gauge spheres

<b>Cr<sub>2</sub>GaC</b> ( 79.3 (9) wt%)	<b>x</b>	<b>y</b>	<b>z</b>	<b>Occupancy</b>	<b>Beq</b>
Cr1	0.3333	0.6667	0.8690	1.00	2.115
Ga1	0.3333	0.6667	0.7500	1.00	2.997
Cl	0.0000	0.0000	0.0000	1.00	1

a /Å	2.89051 (5)
c /Å	12.6053 (4)
a /Å	3.0770 <sup>3</sup>
c /Å	10.9100 <sup>3</sup>
R <sub>Bragg</sub>	0.917
GOF	2.26

**Table S12:** Rietveld refinement parameters of microwave-derived 26-gauge spheres

<b>Cr<sub>2</sub>GaC (72.4 (17) wt%)</b>	<b>x</b>	<b>y</b>	<b>z</b>	<b>Occupancy</b>	<b>Beq</b>
Cr1	0.3333	0.6667	0.8690	1.00	2.115
Ga1	0.3333	0.6667	0.7500	1.00	2.997
Cl	0.0000	0.0000	0.0000	1.00	1
a /Å				2.88380 (10)	
c /Å				12.5815 (8)	
a /Å				3.0770 <sup>3</sup>	
c /Å				10.9100 <sup>3</sup>	
R <sub>Bragg</sub>				2.619	
GOF				2.56	

**Table S13:** Rietveld refinement parameters of microwave-derived 30-gauge spheres

<b>Cr<sub>2</sub>GaC ( 79.3 (13) wt%)</b>	<b>x</b>	<b>y</b>	<b>z</b>	<b>Occupancy</b>	<b>Beq</b>
Cr1	0.3333	0.6667	0.8690	1.00	2.115
Ga1	0.3333	0.6667	0.7500	1.00	2.997
Cl	0.0000	0.0000	0.0000	1.00	1
a /Å				2.89482 (6)	
c /Å				12.6222 (4)	
a /Å				3.0770 <sup>3</sup>	
c /Å				10.9100 <sup>3</sup>	
R <sub>Bragg</sub>				1.513	
GOF				1.56	

## Microsphere SEM/EDS Imaging and Mapping

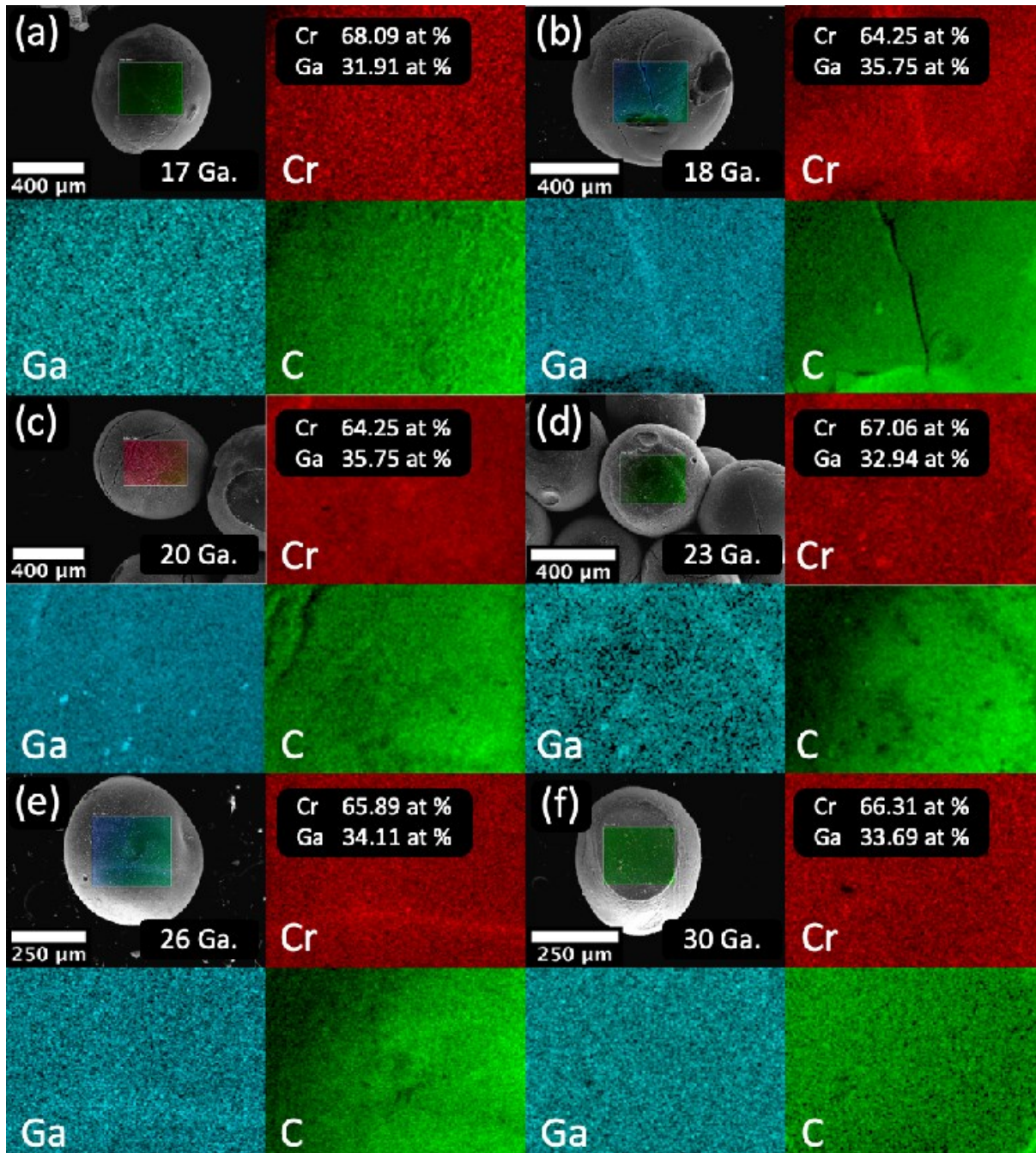


**Fig S14:** EDS data of Furnace spheres (a) 17-gauge (b) 18-gauge (c) 20-gauge (d) 23-gauge (e) 26-gauge (f) 30-gauge



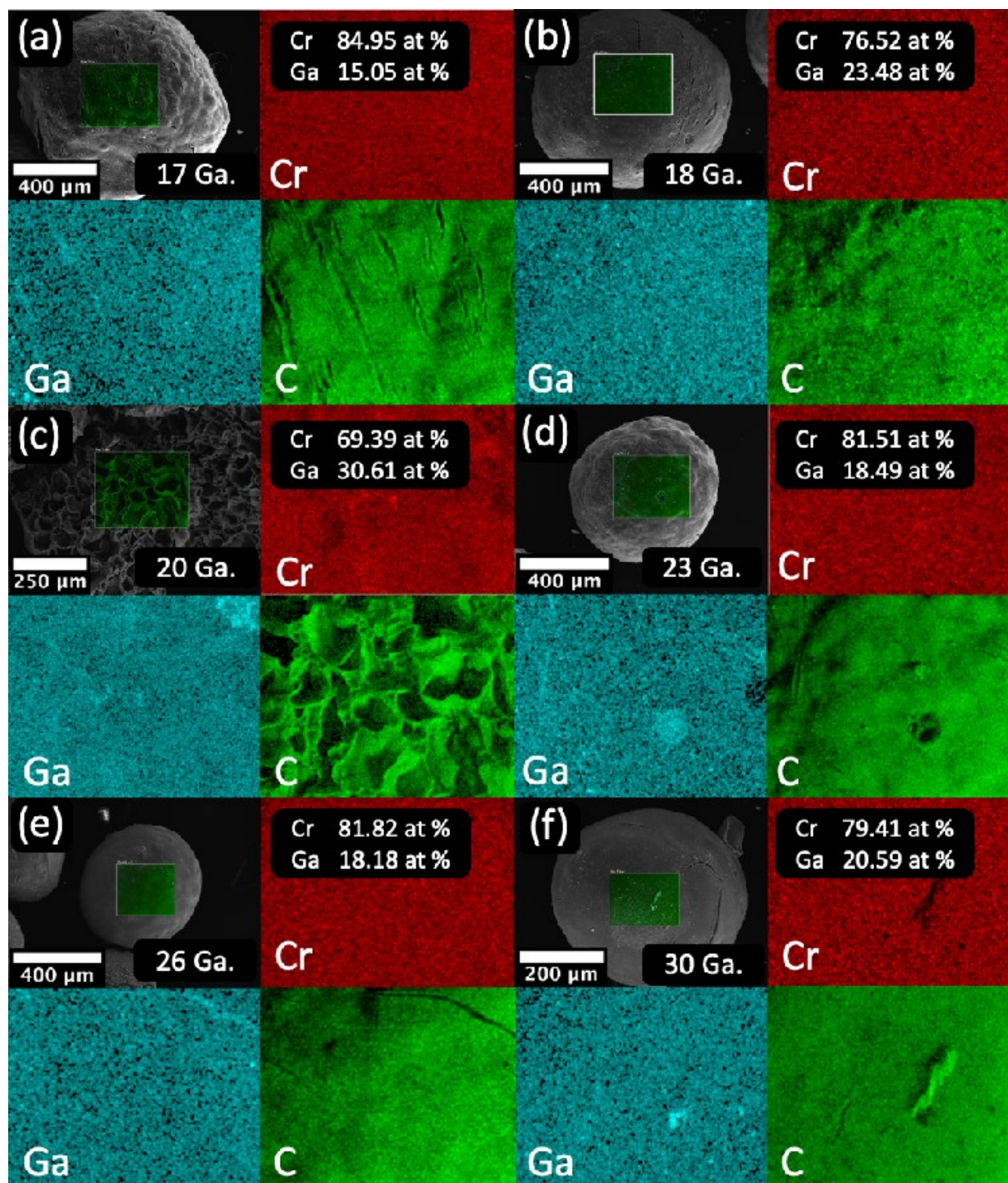


**Fig S15:** EDS data of Microwave spheres (a) 17-gauge (b) 18-gauge (c) 20-gauge (d) 23-gauge (e) 26-gauge (f) 30-gauge

## EDS Map Sum Spectrums

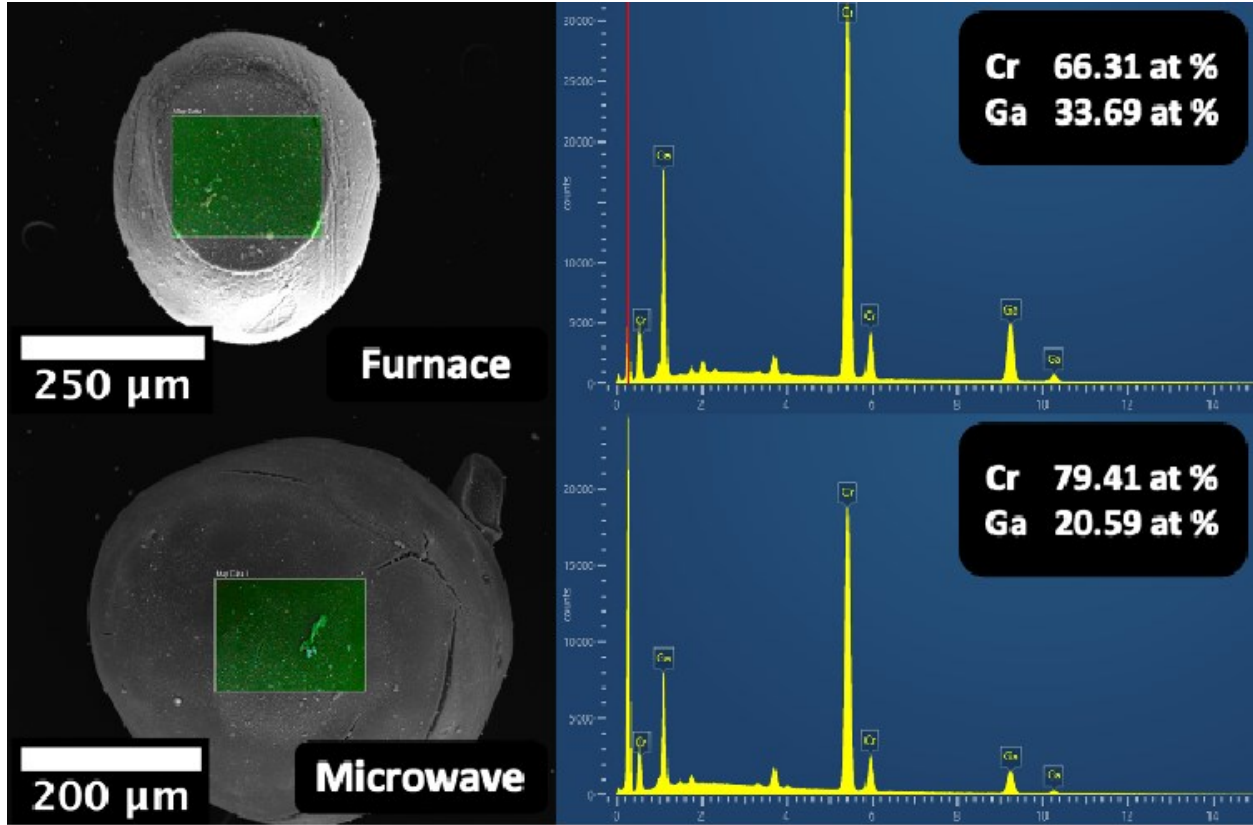


Figure S16. EDS Imaging and Map Sum Spectrums of 17 gauge (furnace and microwave)

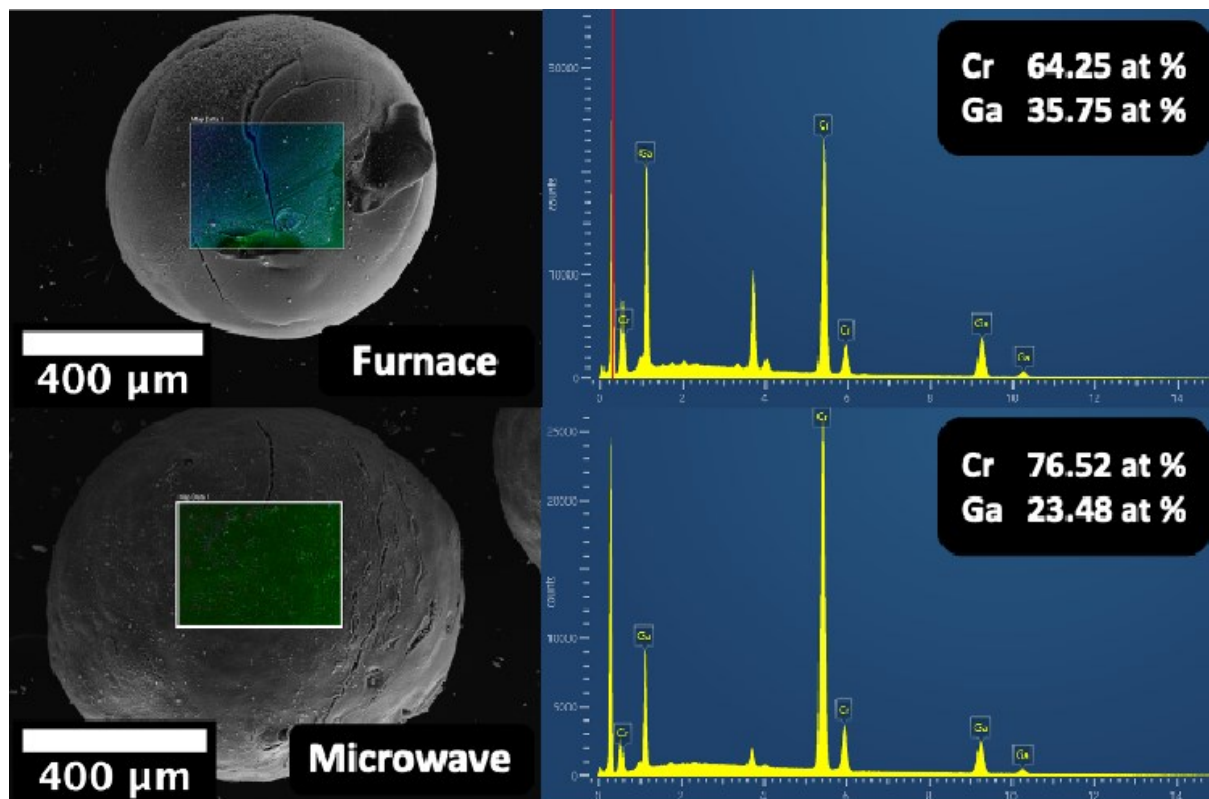


Figure S17. EDS Imaging and Map Sum Spectrums of 18 gauge (furnace and microwave)

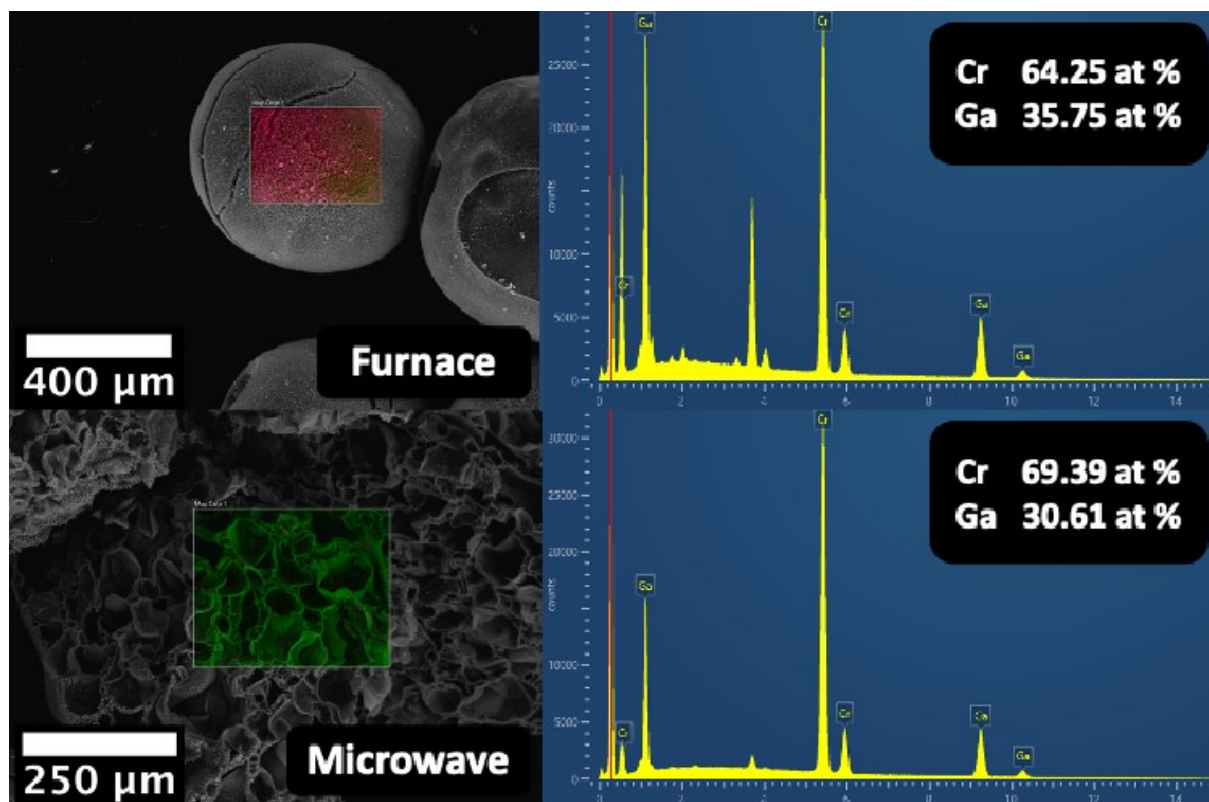


Figure S18. EDS Imaging and Map Sum Spectrums of 20 gauge (furnace and microwave)

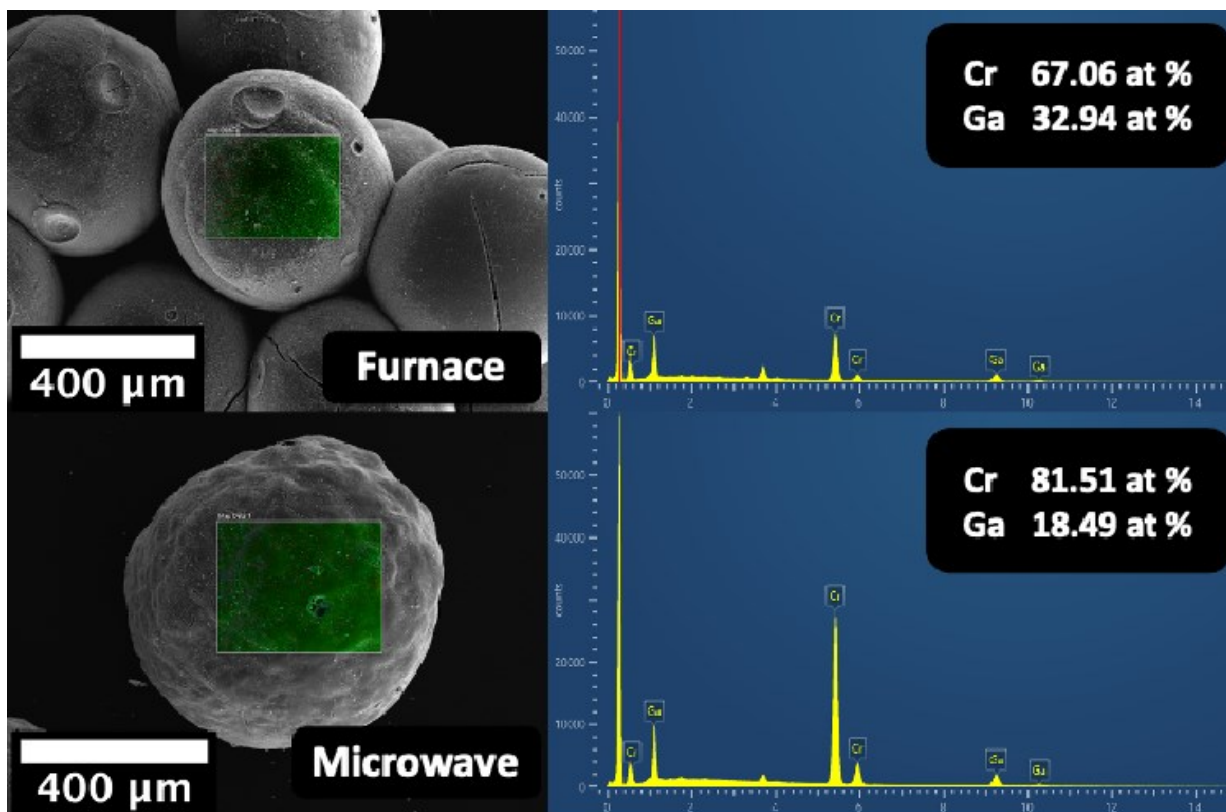


Figure S19. EDS Imaging and Map Sum Spectrums of 23 gauge (furnace and microwave)

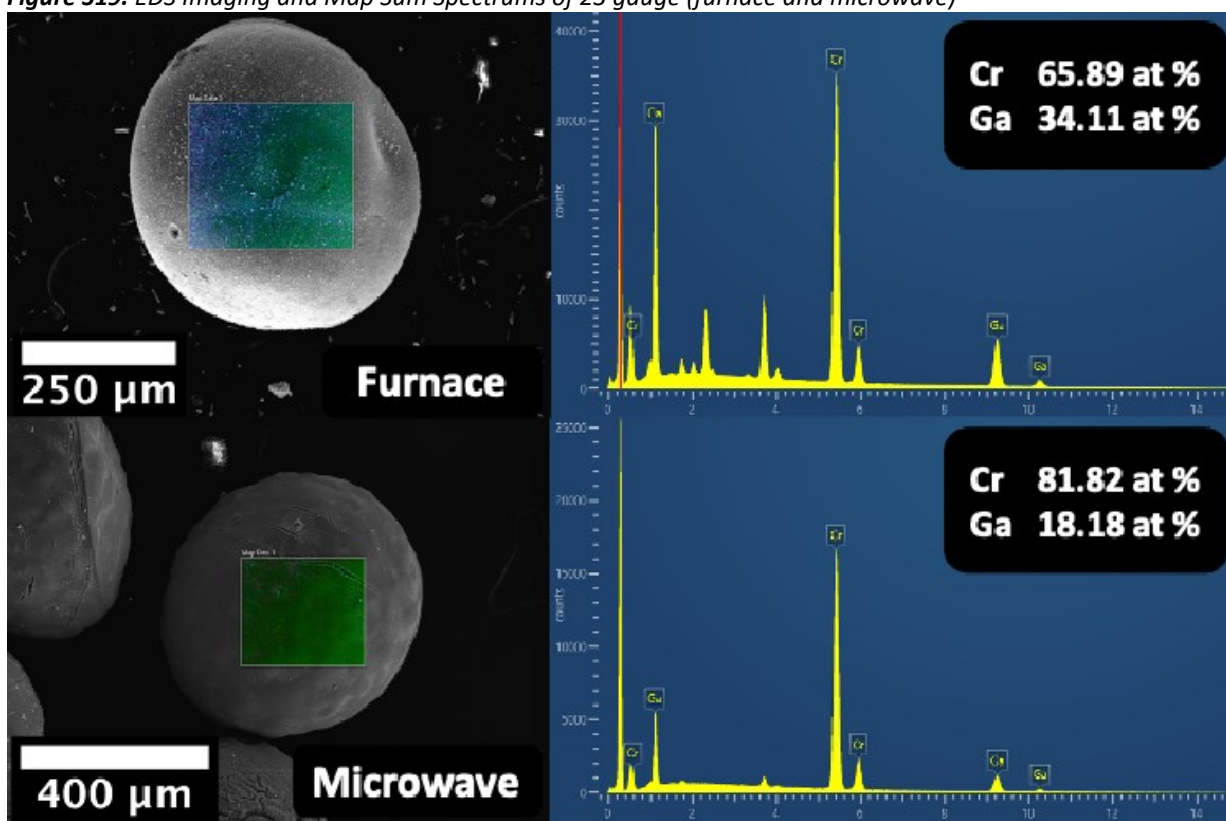


Figure S20. EDS Imaging and Map Sum Spectrums of 26 gauge (furnace and microwave)

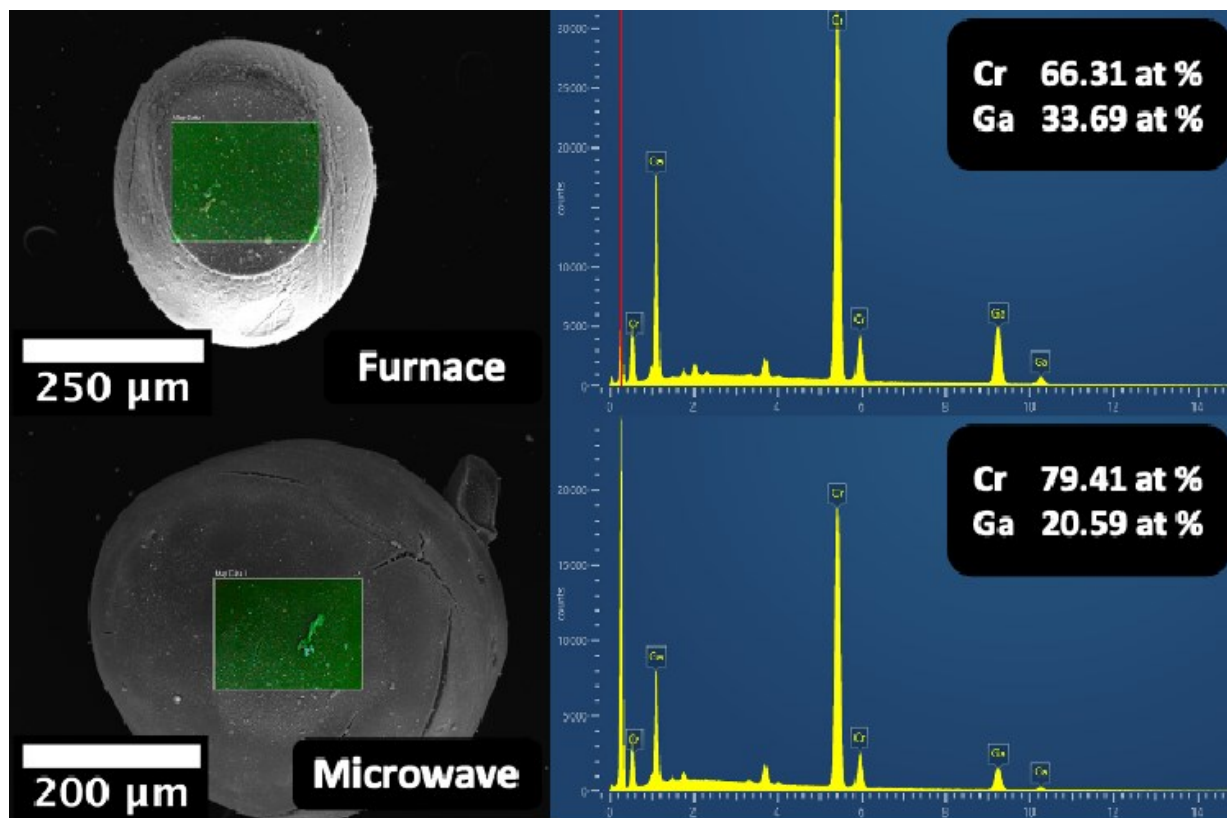


Figure S21. EDS Imaging and Map Sum Spectrums of 30 gauge (furnace and microwave)

### TEM Imaging

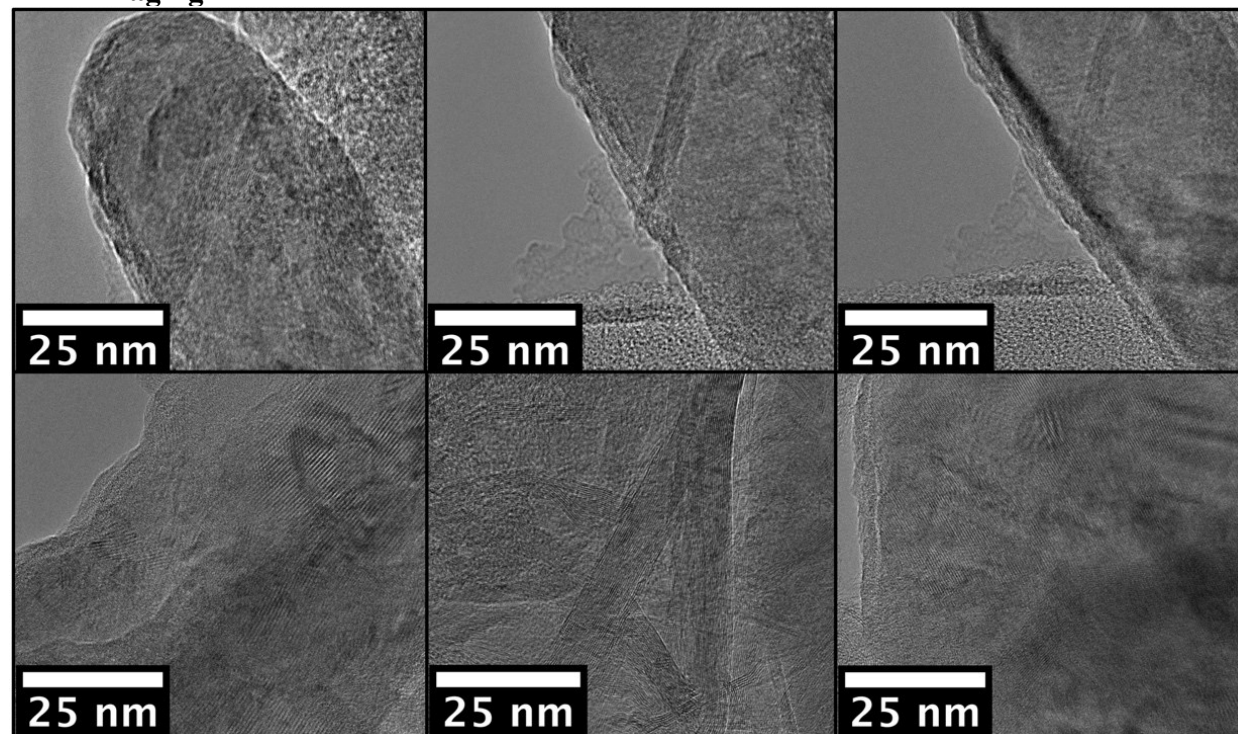
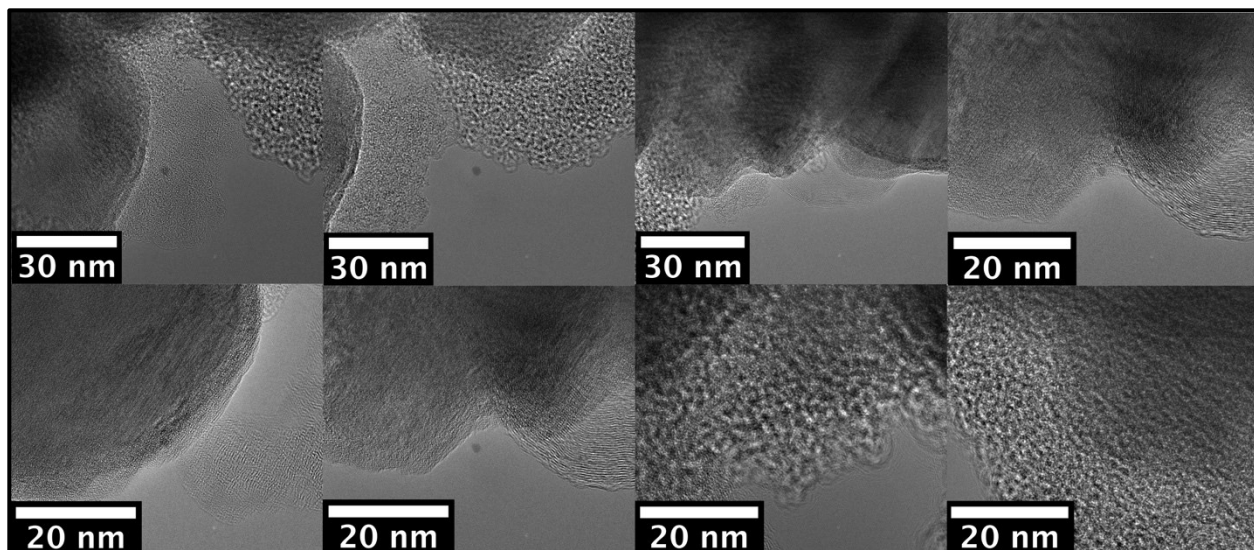
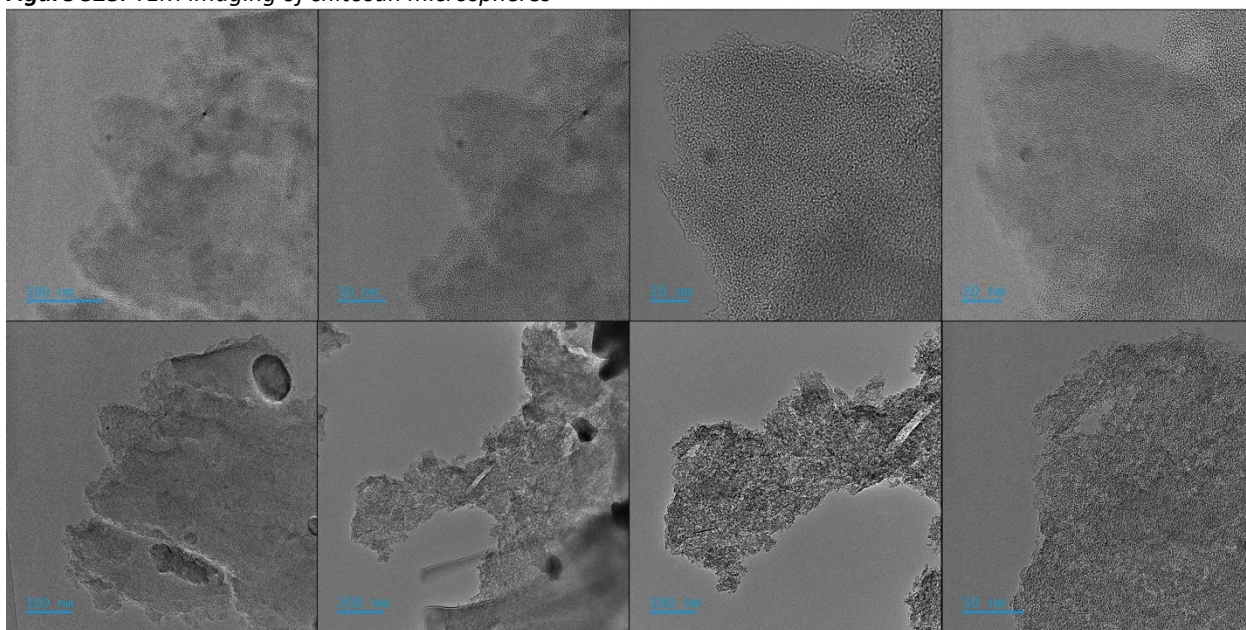


Figure S22. TEM imaging of microwave microspheres



**Figure S23.** TEM imaging of chitosan microspheres



**Figure S24.** HR-TEM imaging of furnace microspheres

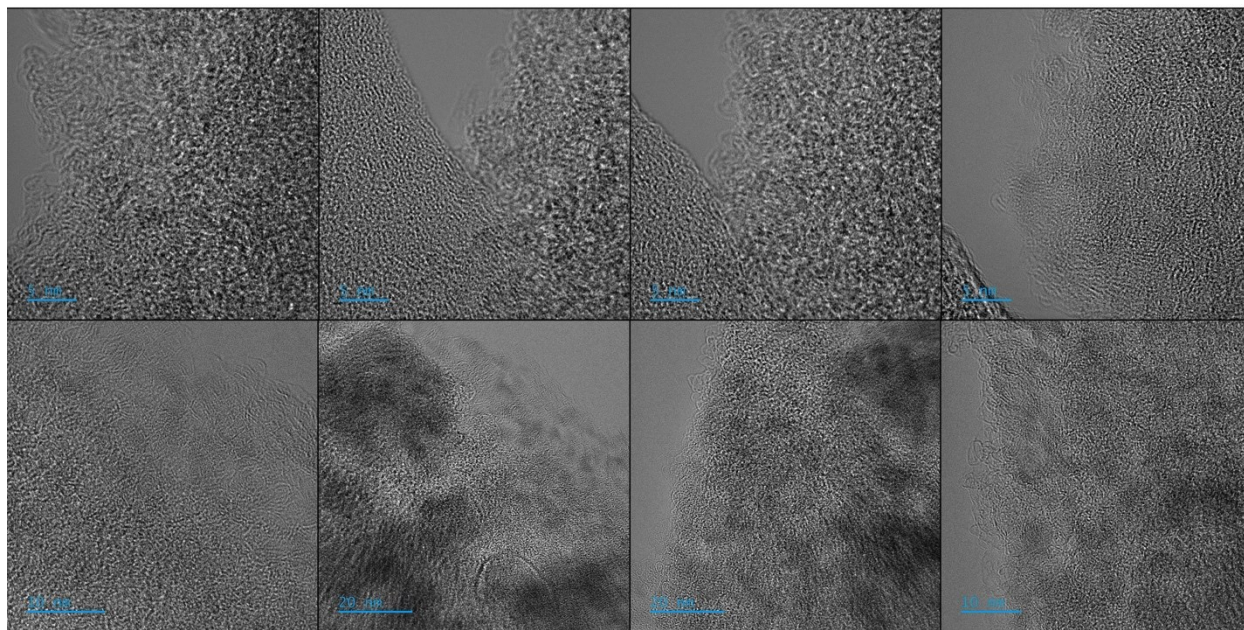


**Figure S25.** HR-TEM imaging of furnace microspheres

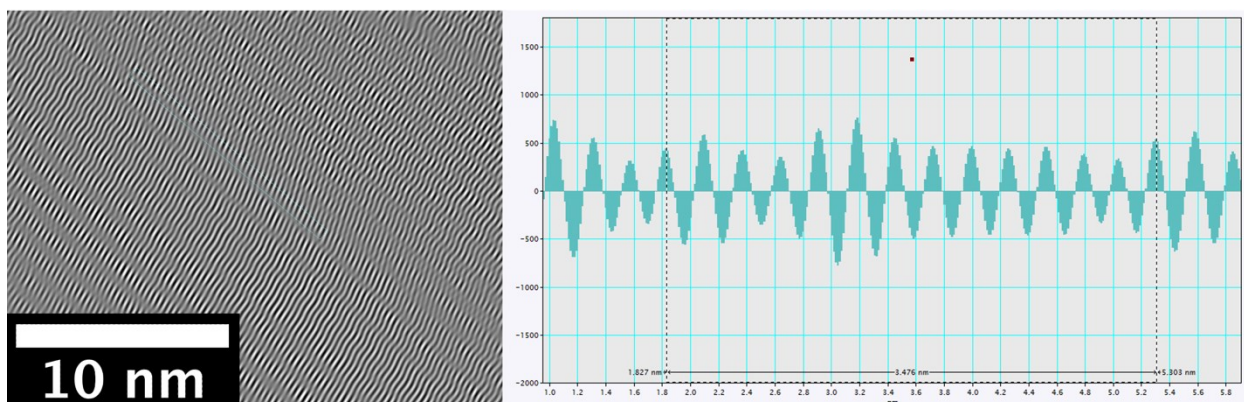


**Figure S26.** Inverse Fourier Transform of HR-TEM imaging of furnace microspheres. Lattice spacing was estimated across 12 different points to get a good average.



**Figure S27.** A depiction of most of the needle gauge sizes used in synthesis.

## References

1. Coelho, A. A. TOPAS and TOPAS-Academic: An optimization program integrating computer algebra and crystallographic objects written in C++: *An. J. Appl. Crystallogr.* **51**, 210–218 (2018).

2. Karlsruhe, I. Inorganic Crystal Structure Database [computer software]. (2022).
3. Villars, P. & Cenzual, K. Pearson's Crystal Structure Data - Crystal Structure Database for Inorganic Compounds (on CD-ROM). (2010).